Accurate modal analysis of microstructured optical fibers with the boundary integral method.

E. Pone, A. Hassani, S. Lacroix and M. Skorobogatiy
Ecole Polytechnique de Montreal, Department de Genie Physique, Montreal H3C 3A7, Canada.
www.photonics.phys.polymtl.ca

Abstract: A boundary integral method for calculating leaky and guided modes of microstructured optical fibers is presented. The method is rapidly converging and can handle a large number of inclusions with arbitrary geometries.

OCIS codes: (060.4005) Microstructured fibers; (290.4210) Multiple scattering

1 Introduction

Microstructured optical fibers (MOFs) have recently attracted much interest because of their unique optical properties [1]. Although significant progress has been made in the modelling of MOFs, rigorous modal analysis remains challenging, especially in the case of large number of holes or non-cylindrical hole shapes. A number of modelling techniques has been developed for finding the modes of MOFs - the plane wave expansion method [2], the localized function method [3] (in a scalar approximation), finite element method [4], boundary element methods [5, 6] and the multipole expansion method [7]. The finite element method requires volume discretization which demands considerable memory resources to achieve high accuracy. It is however well suited to treat complex shapes. The multipole method experiences convergence and accuracy problems when the holes are non circular and too closely spaced from one another. Here, we develop an accurate and efficient boundary integral method for the modal analysis of MOFs. We extend the boundary integral method developed for the modal analysis of conventional waveguides [8]. The key advantages of the proposed method are the following: For circular inclusions much of the calculations are done analytically resulting in a highly accurate and rapidly convergent implementation. The method can treat inclusions of arbitrary shapes defined by a parametrical curve. The method is able to treat accurately systems that contain a large numbers of inclusions even if they are very closely spaced.

2 Description of the method

The schematic of a MOF geometry is shown in Fig. 1(a). The fiber cross-section is located in the xy plane. A finite number N_c of homogeneous inclusions of refractive index n_c are embedded into a background material of refractive index n_g. The field components are taken to have an exp $i(\beta z - \omega t)$ dependence. Here β is the

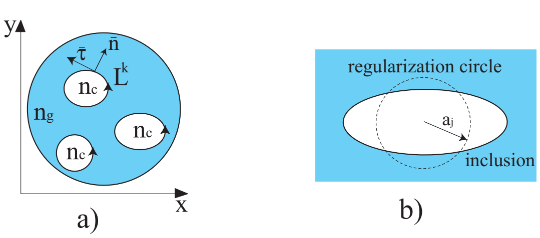

Fig. 1. a) Schematic of a MOF cross section. b) Arbitrary shaped inclusion and the regularization circle.

propagation constant of the mode and ω is the angular frequency, which is related to the free-space wave number by $\omega = ck_0$. The effective index is defined as $n_e = \beta/k_0$. Given the longitudinal components E_z and H_z, all the other field components can be deduced from Maxwells equations. In each of the homogeneous regions, the longitudinal components satisfy the Helmholtz equation: $\nabla^2 E_z^{(c,g)} + {k_0}^2 \gamma_{c,g}^2 E_z^{(c,g)} = 0$ with

$\gamma_{c,g}^2 = n_{c,g}^2 - {n_e}^2$ and similarly for H_z. The longitudinal and tangential components of the fields are continuous:

$$\begin{array}{c} E_z^{(c)} = E_z^{(g)} \qquad H_z^{(c)} = H_z^{(g)} \\ E_t^{(c)} = E_t^{(g)} \Rightarrow \frac{i}{k_0\gamma_c^2}\left(n_e\frac{\partial E_z^{(c)}}{\partial\tau} - \frac{\partial H_z^{(c)}}{\partial n}\right) = \frac{i}{k_0\gamma_g^2}\left(n_e\frac{\partial E_z^{(g)}}{\partial\tau} - \frac{\partial H_z^{(g)}}{\partial n}\right) \\ H_t^{(c)} = H_t^{(g)} \Rightarrow \frac{i}{k_0\gamma_c^2}\left(n_e\frac{\partial H_z^{(c)}}{\partial\tau} + \epsilon_c\frac{\partial E_z^{(c)}}{\partial n}\right) = \frac{i}{k_0\gamma_g^2}\left(n_e\frac{\partial H_z^{(g)}}{\partial\tau} + \epsilon_g\frac{\partial E_z^{(g)}}{\partial n}\right) \end{array}, \tag{1}$$

where $\frac{\partial}{\partial\tau}$ is the tangential derivative to the boundary contour L, $\frac{\partial}{\partial n}$ is the outer normal derivative, and $\epsilon_{(c,g)}$ is the dielectric constant of either the inclusion or the cladding. Since E_z and H_z satisfy the Helmholtz equation, they can be represented by the following contour integrals [8]:

$$E_z(\vec{r}) = \int_L e(\vec{r}_s)G(\vec{r},\vec{r}_s)dl_s \qquad H_z(\vec{r}) = \int_L h(\vec{r}_s)G(\vec{r},\vec{r}_s)dl_s \tag{2}$$

Evaluating the contour functions $e(\vec{r}_s)$ and $h(\vec{r}_s)$ is sufficient to obtain the electromagnetic fields. The function $G(\vec{r},\vec{r}_s)$ is the Green's function of the Helmholtz equation: $G(\vec{r},\vec{r}_s) = \frac{i}{4}H_0^{(1)}(k_0\gamma|\vec{r}-\vec{r}_s|)$ where $H_0^{(1)}()$ is the zeroth-order Hankel function of the first kind. If $\vec{r}$ is located inside of an inclusion the integration is taken along the inclusion's boundary while if it is located in the fiber cladding the integration is taken along all the inclusions boundaries. Inserting the contour integrals (2) into the continuity conditions (1), a system of four coupled linear integral equations for the contour functions $e_c^{(k)}$, $e_g^{(k)}$, $h_c^{(k)}$, $h_g^{(k)}$, $k = 1 \dots N_c$, is obtained. The value of n_e, for which a nontrivial solution exists, defines the effective refractive index of the fiber mode.

Consider first the circular inclusions. Let $\psi^{(k)}(s')$ represent any of the contour functions $e_c^{(k)}$, $e_g^{(k)}$, $h_c^{(k)}$, or $h_g^{(k)}$ and let $s_t = t\frac{2\pi}{2n^{(k)}}$, $t = 0,\dots,2n^{(k)}-1$, be an equidistant grid. For the discretization of the integral equations, we use the trigonometric interpolation: $\psi^{(k)}(s') \approx \sum_{t=0}^{2n^{(k)}-1}\left(\frac{1}{2n^{(k)}}\sum_{m=-n^{(k)}}^{n^{(k)}-1} e^{im(s'-s_t)}\right)\psi^{(k)}(s_t)$. With this expression, all the integrals take the following form: $\sum_{t=0}^{2n^{(j)}-1}\left(\frac{1}{2n}\sum_{m=-n^{(j)}}^{n^{(j)}-1} e^{-ims_t}\int_0^{2\pi} e^{ims'}\Phi(s,s')ads'\right)\psi^{(j)}(s_t)$ where a stands for the inclusion radius and $\Phi(s,s')$ stands for $G(s,s')$, $\dfrac{\partial G(s,s')}{\partial n}$ or $\dfrac{\partial G(s,s')}{\partial\tau}$. The fourier transforms of $\Phi(s,s')$ in the case of a contour containing the singular point $\vec{r}_{s'} = \vec{r}_s$, which seems to be the most problematic, can be evaluated analytically according to the following formulas [9]: $\int_0^{2\pi} e^{ims'}G(s,s')ds' = \frac{i\pi}{2}J_m(k_0\gamma a_j)H_m^{(1)}(k_0\gamma a_j)e^{ims}$, $\int_0^{2\pi} e^{ims'}\frac{\partial G(s,s')}{\partial\tau}ds' = -\frac{m\pi}{2a_j}J_m(k_0\gamma a_j)H_m^{(1)}(k_0\gamma a_j)e^{ims}$ and $\int_0^{2\pi} e^{ims'}\frac{\partial G(s,s')}{\partial n}ds' = \left[-\frac{1}{2a_j} + \frac{ik_0\gamma\pi}{2}J'_m(k_0\gamma a_j)H_m^{(1)}(k_0\gamma a_j)\right]e^{ims}$, where $J_m()$ and $H_m^{(1)}()$ are the mth order Bessel and the first kind Hankel functions, while a prime denotes the derivative with respect to the argument. For the integrals along the other contours which have no singularities a FFT is performed. If the distance between the source point $\vec{r}_s$ and a contour which does not contain this point is relatively large (in the case of a large number of inclusions, this becomes the most common situation) a simple trapezoidal rule is applied instead of the trigonometric interpolation, resulting in a very efficient method. For the arbitrary shaped inclusions, the discretization procedure is similar to the one used for the circular inclusions except for the evaluation of the fourier transform of $\Phi(s,s')$ along a contour containing the singular point where a regularization procedure is performed. At the arbitrary inclusion, a circle with a comparable diameter as shown schematically in Fig. 1(b) is constructed. To the integrals along the arbitrary inclusion the corresponding integrals along the regularizing circle are substracted and added. The substraction makes these integrals nonsingular while the added part is evaluated analytically according to the previous formulas.

When the discrete integrals are substituted into integral equations, a matrix equation is obtained: $A(n_e)\cdot X = 0$. The vector of unknowns X has $4N_c\sum 2n^{(k)}$ elements which are the values of $e_c^{(k)}(s_t)$, $e_g^{(k)}(s_t)$, $h_c^{(k)}(s_t)$, $h_g^{(k)}(s_t)$, $k = 1,\dots,N_c$. The effective index is obtained by the values of n_e for which the determinant of $A(n_e)$ is zero. We perform a search for the minima of the determinant along a single line in the complex plane and then use these local minima as initial values for a further root refinement with the Newton method. An important part of the method is the inclusion of the symmetries. Considerable reduction of the overall computational cost is achieved as only a small part of a structure has to be used in a simulation.

The method was first tested on several simple problems, and it shows excellent agreement with simulations performed by the multipole method. As a first example we consider finding the fundamental core guided mode of a hollow-core MOF presented in Fig. 2(a). It consists of five rings of circular holes arranged on a hexagonal lattice and surrounding a hollow core formed by the two missing rings in the fiber center. The hole to hole pitch is $\Lambda = 2.74\mu$m, the hole diameter is $d = 0.95\Lambda$, and the core diameter is $d_c = 2.5d$. The glass cladding has a refractive index of $n_g = 1.45$, while for the air holes $n_c = 1$. Dispersion curves for the fundamental core guided mode of this fiber are shown in Fig. 2(a). Next, the structure presented in Fig. 2(b)

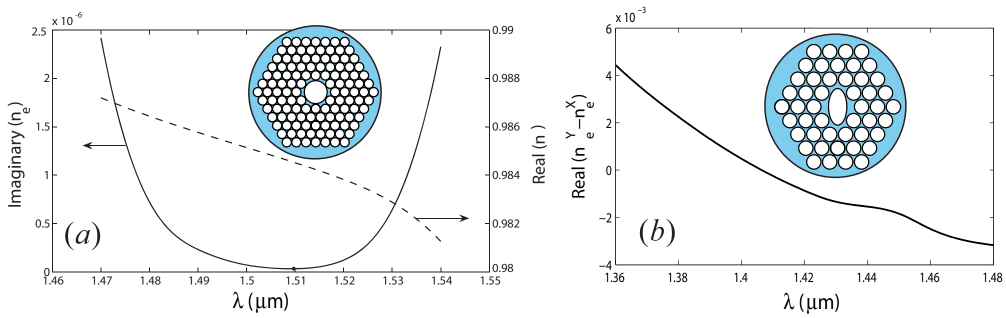

Fig. 2. (a) Dispersion curve of the fundamental mode of a hollow core MOF with 5 rings of holes. (b) Birefringence of the fundamental mode of a MOF with a elliptic hollow core.

is considered. It consists of three layers of circular holes and a central elliptic core. The hole pitch is $\Lambda = 2\mu m$, the hole diameter is $d = 0.9\Lambda$, and the elliptical core has axis $a = 2.3\mu m$ and $b = 4.6\mu m$. The glass cladding is assumed to have refractive index of $n_g = 1.45$, while refractive index of the air holes is $n_c = 1$. In Fig. 2(b) the birefringence of the fundamental mode of this fiber is presented. Interestingly, the birefringence changes its sign around $\lambda = 1.41\mu m$.

3 Conclusion

A high performance boundary integral method for the modal analysis of MOFs is presented. The method can treat a large number of arbitrary shaped inclusions. When spacing between inclusions decreases no convergence problems arise; only the computational cost of some of the matrix elements (the order of FFT) increases. For circular inclusions, in particular, the majority of the calculations are done analytically, ensuring high accuracy and rapid convergence.

References

1. P. Russell "Photonic crystal fibers," Science **299**, 358-362 (2003).
2. A. Ferrando, E. Silvestre, J.J. Miret, P. Andres and M.V. Andres "Full vector analysis of a realistic photonic crystal fiber," Opt. Lett. **24**, 276-278 (1999).
3. T.M. Monro, D.J. Richardson, N.G.R. Broderick and P.J. Bennett "Holey optical fibers: an efficient modal model," J. Lightwave Technol. **17**, 1093-1102 (1999).
4. K. Saitoh, M. Koshiba, "Full-Vectorial Imaginary-Distance Beam Propagation Method Based on a Finite Element Scheme: Application to Photonic Crystal Fibers," IEEE J. Quantum Electron. **38**, 297 (2002).
5. T. Lu and D. Yevick, "A vectorial boundary element method analysis of integrated optical waveguides," J. Lightwave Technol. **21**, 1793-1807 (2003).
6. H. Cheng, W. Crutchfield, M. Doery, and L. Greengard, "Fast, accurate integral equation methods for the analysis of photonic crystal fibers I: Theory," Opt. Express **12**, 3791-3805 (2004).
7. T. P. White, B. T. Kuhlmey, R. C. McPhedran, D. Maystre, G. Renversez, C. Martijn de Sterke and L. C. Botten "Multipole method for microstructured optical fibers. I. Formulation," J. Opt. Soc. Am. B **19**, 2322-2330 (2002).
8. S. V. Boriskina, T. M. Benson. P. Sewell and A. I. Nosich "Highly efficient full-vectorial integral equation solution for the bound, leaky and complex modes of dielectric waveguides," IEEE J. Sel. Top. Quantum Electron. **8**, 1225-1231 (2002).
9. S. V. Boriskina, P. Sewell and T. M. Benson "Accurate simulation of two-dimensional optical microcavities with uniquely solvable boundary integral equations and trigonometric Galerkin discretization," J. Opt. Soc. Am. A **21**, 393-402 (2004).